Received May 13, 2019, accepted June 17, 2019, date of publication June 24, 2019, date of current version July 12, 2019.

Digital Object Identifier 10.1109/ACCESS.2019.2924531

Performance Enhancement of an Orbital-Angular-Momentum-Multiplexed Free-Space Optical Link Under Atmospheric Turbulence Effects Using Spatial-Mode Multiplexing and Hybrid Diversity Based on Adaptive MIMO Equalization

BEDIR BEDIR YOUSIF[1] AND EBRAHIM ELDESOKY ELSAYED[2]

[1]Department of Electronics and Communications Engineering, Faculty of Engineering, Kafrelsheikh University, Kafrelsheikh 35514, Egypt
[2]Department of Electronics and Communications Engineering, Faculty of Engineering, Mansoura University, Mansoura 35516, Egypt

Corresponding author: Ebrahim Eldesoky Elsayed (engebrahem16@gmail.com)

ABSTRACT In this paper, we propose an adaptive multiple-input–multiple-output (MIMO) free-space optical (FSO) links using an orbital-angular-momentum (OAM)-multiplexed based on the spatial-mode multiplexing (SMM) through the turbulent channel. We propose to use the SMM and spatial-mode diversity (SMD) combined with an adaptive MIMO technique to mitigate the atmospheric turbulence effects. In this paper, our objective is to design the adaptive MIMO–FSO links based on OAM–MIMO/SMM multiplexed and analyze its performance in the atmospheric turbulence conditions. The simulation results show four OAM modes-based MIMO/SMM and resulting in four OAM-multiplexed channels. Each OAM mode carries a 100-Gbit/s quadrature phase-shift keying signal (aggregate 400 Gbit/s) on a single wavelength channel ($\lambda \sim 1550$ nm) and is transmitted for a 2-km link. The calculated received power and inter-channel crosstalk of an OAM–MIMO/SMM signal fluctuate by 4.5 –6 dB, respectively. The *power penalties* can be reduced by 1–4 dB for all channels after OAM–MIMO/SMM equalization at a bit-error rate (BER) of 10^{-9}. The calculating results show that the system using an OAM-based MIMO/SMM and SMD multiplexing achieves superior BER performance using an adaptive MIMO/SMM equalization. The Numerical results show favorable transmission performance of OAM based on MIMO/SMM and the SMD multiplexing compared to the conventional-MIMO (CMIMO) of FSO transmission link. The Simulation models verified the superior BER performance of OAM–SMD-based MIMO/SMM. The SMM/MIMO–SMD technique performed better in the channel capacity and signal-to-noise ratios over other commonly used CMIMO algorithms. To sufficiently discuss the OAM–MIMO/SMM behavior-based SMD multiplexing, the performance of the novel SMM/MIMO–SMD technique is analyzed using simulations based on the Matlab/simulink program in order to verify the accuracy of the models and simulation results. This paper could be useful for the practical implementation of the SMM and the SMD using an adaptive MIMO equalization in the FSO systems.

INDEX TERMS Free-space optical communications, adaptive MIMO equalization, orbital-angular-momentum-multiplexed, spatial-mode multiplexing (SMM), power penalty (PP), spatial-mode diversity (SMD).

I. INTRODUCTION

Free-space optical (FSO) communication systems can potentially benefit from the transmission of multiple spatially orthogonal beams and orbital-angular-momentum (OAM)-multiplexed beams through a single aperture pair where the channel capacity is multiplied by the number of OAM modes [1]–[7]. There are several ways to mitigate the power penalty (PP) and inter-channel crosstalk (ICC), including wave-front sensor or wave-front sensorless based

The associate editor coordinating the review of this manuscript and approving it for publication was Honglong Chen.

adaptive optics (AO) systems [8]–[10], adaptive multiple-input and multi-output (MIMO) techniques [11]–[13], and forward error correction (FEC) based channel coding techniques [14]–[16]. Spatial-mode multiplexing (SMM) in an FSO communication is the counterpart of the mode-division multiplexing (MDM) that has recently attracted a fair amount of attention to increase the channel capacity [1], [17]. One approach is to use the well-MIMO techniques, for which multiple aperture sizes are employed at the transmitter and the receiver [18]. SMM is to use MIMO-based multiple OAM as an additional effective degree of freedom (EDOF) has been investigated in [18]. SMM has the potential of achieving high EDOF for communication. In this work, we developed the proposed system of [18] using the SMM and spatial-mode diversity (SMD) in OAM–MIMO to increase the link robustness and system capacity. We proposed a novel case for four OAM–MIMO/SMM modes, the resulting in four OAM channels. Each OAM mode carries a 100 Gbit/s quadrature phase-shift keying (QPSK) signal on a single wavelength channel ($\lambda \sim 1550$ nm) is transmitted for a 2 km link. The optimal sets of OAM state numbers are determined at each value of the signal-to-noise ratio (SNR) and turbulence strength considered. However, the SMM distribution of the OAM state is susceptible to aberrations caused by the atmospheric turbulence (AT) effects [19]–[21]. When beams-carrying OAM and MIMO-based SMM multiplexing are transmitted in the FSO links, the AT will modify the phase structure of OAM modes, the power of one OAM state spread to the other OAM states [19]. Recently, the adaptive optics and channel coding are commonly used to mitigate the AT effects of an OAM-based MIMO multiplexed FSO communication links. For example, I.B. Djordjevic and Z. Qu demonstrated a turbulence mitigation scheme by a low-density parity check (LDPC) coded OAM-based transmission system and an AO [22], [23]. Using this model, we maximize the overall channel capacity for the optimal set of OAM mode numbers [24], [25]. We analyze the performance of FSO communication link using an OAM–MIMO/SMM beam based on an adaptive MIMO equalization with non-zero radial index [26]. Also, we use OAM–MIMO/SMM which carries by a Laguerre–Gaussian (LG) beam, is described by its nonnegative integerρ and an azimuthal integer l $\left(\text{i.e., } LG_{\rho,l}\right)$ [27]. Previous works describing the use of OAM-multiplexed data channels have typically shown data transmission using $\rho = 0$ beams of different l [3]. In this paper, we explore the use of LG beams with $\rho > 0$ in OAM–MIMO/SMM multiplexed FSO communication links. Through simulation and modeling, we investigate the power loss incurred by the beam divergence and limited-size receiver apertures. In this work, we discuss the performance of LG beams with $\rho > 0$ in OAM–MIMO/SMM. The simulation results show that $\rho = 0$ beams is lower as compared to $\rho > 0$ beams with receiver aperture sizes and the received power under certain 2 km that has the same l value. Simulation results show that in 2 km OAM–MIMO/SMM-based FSO links, using transmitter lenses to focus OAM–MIMO/SMM beams could reduce power loss for higher-order OAM beams by more than 12 dB in both links [28]. For system robustness, we investigate the effect of using transmitter lenses under conditions of link misalignment (i.e., receiver angular error (RAE) or lateral displacement between the transmitter and receiver). In this study, we discuss the high-speed OAM–MIMO/SMM multiplexed FSO communication systems, enabled by enabled by AO, LDPC coding, spatial diversity and adaptive MIMO equalization. In addition, we demonstrate the PP mitigation for 4×4 OAM modes using an adaptive MIMO equalization combined with the SMM and SMD of an OAM–MIMO/SMM techniques [12]. The simulation results show that under the weak turbulence (WT) using four OAM–MIMO/SMM could help recover system bit-error rate (BER) with PP of 1 dB -4 dB for all channels after OAM–MIMO/SMM equalization [12], [29]. In this paper, we discuss the design guidelines and technical challenges for achieving good performance in an OAM-multiplexed FSO communication link using OAM–MIMO/SMM and the novel SMM/MIMO-SMD technique. The remaining part of this paper is organized as follows. Section **II** discusses the proposed scheme along with a mathematical model of OAM–MIMO/SMM in the FSO communication link. The performance of the power penalty is analyzed in Section **III**. In Section **IV,** the numerical results and discussions of the proposed system are reported. Finally, Section **V** concludes the paper and discusses future work.

II. SYSTEM MODELING

Fig. 1 shows the concept and model simulating the use of the proposed system in an OAM-multiplexed data link. The proposed system of OAM based on an adaptive MIMO/SMM and SMD multiplexed data links in the FSO system as shown in Fig. 1 (b). In our simulation, the system PP could be reduced using the mode spacing (MS), multiple aperture sizes, power loss, and ICC. The collimated Gaussian beams (GBs) are carrying independent data streams at the wavelength $\lambda \sim 1550$ nm. Spiral phase plate (SPP) converts the data carrying GBs into OAM-MDM beam. Multiple OAM–MIMO/SMM beams are then multiplexed and passed through a pair of T_x lenses (f_1 and f_2) before transmitting in the FSO link. The equivalent focal lengths f_1 and f_2 of the lens pair f_0 satisfies $1/f_0 = 1/f_1 + 1/f_2 - d_f/f_1 f_2$, where the lens-spacing offset Δ defined as $f_1 + f_2 - d_f$, with d_f representing the center-to-center spacing between these two lenses [28]–[31]. In our simulation, we use these transmitter (T_x) lenses to focus OAM beams at the receiver by tuning offset Δ and the spacing between those two lenses was adjustable such that the equivalent focal length was tunable. Careful design of the transmitter lenses could help reduce power loss, but it is also useful to know its effect on the robustness of an OAM-multiplexed FSO link under angular error or displacement [28]. To sufficiently discuss the OAM–MIMO/SMM behavior based SMD multiplexing, the performance of the novel SMM/MIMO–SMD technique

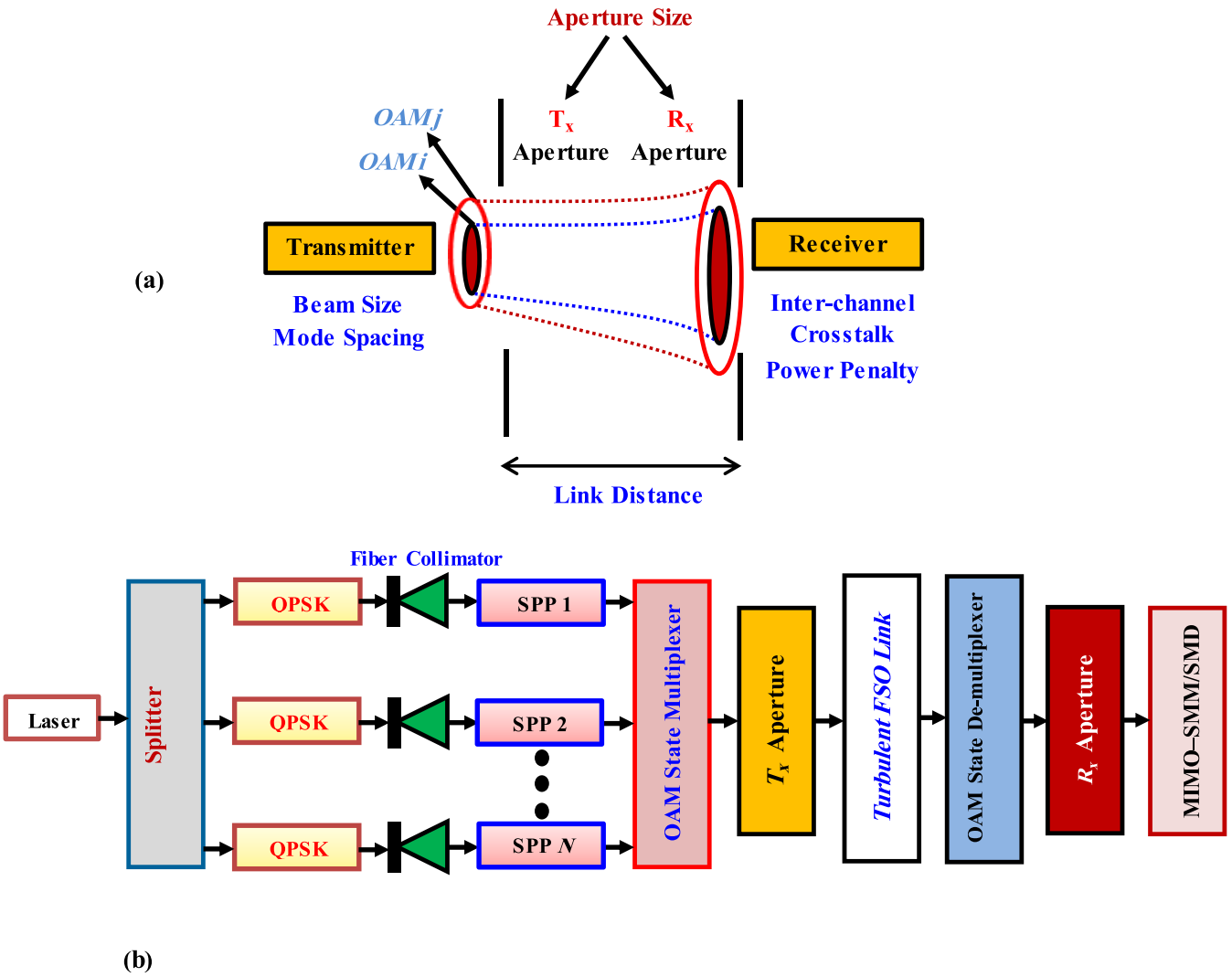

FIGURE 1. Simulation schematic of an OAM-multiplexed data link (a) concept of an OAM-multiplexed and (b) the proposed system of OAM based on an adaptive MIMO/SMM and SMD multiplexed data links in the FSO system.

is analyzed using simulations based on Matlab/Simulink Program in order to verify the accuracy of models, simulation results are compared with those obtained from [18]. The algorithm is validated by the program developed by Matlab, and the results show that the model can be accurately and effectively supported.

A. ATMOSPHERIC TURBULENCE MITIGATION BASED ON AN ADAPTIVE MIMO/SMM

In this section, we first briefly describe the OAM–MIMO/SMM multiplexed in the FSO links under the AT. After that OAM–MIMO/SMM transmits through the AT and additive white Gaussian noise (AWGN) channel, the received OAM–MIMO/SMM-multiplexed beams are deformed, after OAM–MIMO/SMM beam de-multiplexer and OAM–MIMO/SMM state converter, the output signal matrix $\widehat{\mathrm{S}} = \left[\widehat{\mathrm{S}}_1(n), \widehat{\mathrm{S}}_2(n), \ldots, \widehat{\mathrm{S}}_N(n)\right]^T$ can be shown as [32]–[34]

$$\widehat{\mathrm{S}} = \mathrm{HS}, \tag{1}$$

where the transmitted signal $\mathrm{S} = [\mathrm{S}_1(n), \mathrm{S}_2(n), \ldots, \mathrm{S}_N(n)]^T$, T denote matrix response, H is the $N \times N$ AT matrix with $h_{i,j}, i, j \in [1, N]$. After OAM–MIMO/SMM multiplexing, the output signal $\mathrm{Y} = \left[\mathrm{y}_1(n), \mathrm{y}_2(n), \ldots, \mathrm{y}_N(n)\right]$ is shown as

$$\mathrm{Y} = \mathrm{G}\widehat{\mathrm{S}}, \tag{2}$$

where G is the *OAM-MIMO/SMM* matrix with $g_{i,j}, i, j \epsilon [1, N]$. The estimation SNRs $\hat{\mathrm{y}}_j(n), j \epsilon [1, N]$ is the estimation of $\hat{\mathrm{s}}_i(n)$, which can be expressed as

$$\hat{\mathrm{y}}_j(n) = \sum_{i=1}^{N} \sum_{l=0}^{L} w_{i,j}^{l}(n) \widehat{\mathrm{s}}_i(n-l), \tag{3}$$

where $w_{i,j}^{l}$ is the tap gain coefficient of OAM–MIMO/SMM equalization, and $L+1$ is the length of tab coefficient.

B. AN OAM–MIMO/SMM WITH SPATIAL-MODE DIVERSITY

In our analysis, an OAM–MIMO/SMM multiplexed beam $\mathrm{U}(w_z, \theta)$ can be formed by a SPP $\exp(il\theta)$ to GB

$$\mathrm{U}(w_z, \theta) = \mathrm{A}(w_z) \cdot \exp(il\theta), \tag{4}$$

where $\mathrm{A}(w_z) \propto \exp\left(-w_z^2/w_0^2\right)$ is the electric field amplitude at the waist of GB, w_z is the beam radius at the transmission distance of z, and w_0 is the beam waist. After QPSK modulation, the hybrid light field distribution of N OAM–MIMO/SMM-multiplexed beams is given by [3]

$$U_{MUX}(w_z, \theta, t) = \sum_{s=1}^{N} m_s(t) \cdot A_s(w_z) \cdot exp(il_s\theta), \tag{5}$$

where l_s is the topological quantum number which is distinctive by the angle mark of s, $A_s(w_z)$ represents the electric field amplitude and is different with various l_s.$m_s(t)$ represents the QPSK signal of OAM–MIMO/SMM channel s, which can be written as [33]

$$m_s(t) = \alpha \cdot exp(\omega \cdot t + i\psi_s), \psi_s \epsilon \left\{\frac{\pi}{4}, \frac{3\pi}{4}, \frac{5\pi}{4}, \frac{7\pi}{4}\right\}, \tag{6}$$

where α is the signal amplitude and ω is the angular frequency of OAM–MIMO/SMM beams. ψ_s denotes the signal phase of OAM–MIMO/SMM channel s, and t is the axis of time. With a total power, $r_k = P_{+\mathrm{m}} + P_{-\mathrm{m}} = |U_1|^2 + |U_2|^2$, power ratio between one beam and the total power, $\alpha_N = \sqrt{P_{+m}/r_k}$, and a relative phase shift between the two beams, φ_L, expressed as [34]

$$\begin{aligned} &S_{KNL}(r_k, \alpha_N, \varphi_L, t) \\ &= U_1(r_k, \alpha_N, \varphi_L, t) + U_2(r_k, \alpha_N, \varphi_L, t) \\ &= \sqrt{r_k g(t) \alpha_N^2} \exp(im\psi) \exp\left(-\frac{i\varphi_L}{2} g(t)\right) \\ &\quad + \sqrt{r_k g(t)\left(1-\alpha_N^2\right)} \exp(-im\psi) \exp\left(\frac{i\varphi_L}{2} g(t)\right), \end{aligned} \tag{7}$$

In this case, *g(t)* is GB pulse for the amplitude and signal phase.

$$P(\mathrm{t}) = \sum_{n} S_{KNL}(r_k, \alpha_N, \varphi_L, t) * \delta(t - nT). \tag{8}$$

where $P(\mathrm{t})$ is the pulse train, $S_{KNL}(r_k, \alpha_N, \varphi_L, t)$ is the coherent coupling in the optical light field. At the link distance of z, the radius of a $LG_{\rho,l}$ beam could be characterized as [27], [30]

$$w_z = w_0\sqrt{2\rho + l + 1}\sqrt{1 + \left(\frac{\lambda z}{\pi w_0^2}\right)^2}, \tag{9}$$

where λ is the wavelength, the received field can then be written as [35]

$$\varphi(r, z) = \sum_{i=-\infty}^{+\infty} \sum_{k \epsilon N} \rho_k \alpha_{ki} u_i(r, z) \tag{10}$$

After the SMM de-multiplexing, for the photo-detector collecting the power in the SMD state $\boldsymbol{i}$, the received power is given by [35]

$$y_i = \int \left|\sum_{k \epsilon N} \rho_k \alpha_{ki} u_i(r, z)\right|^2 dr = \left|\sum_{k \epsilon N} \rho_k \alpha_{ki}\right|^2, \tag{11}$$

In Eq. (11), the signal and ICC are coherently superimposed, thus for the whole SMM system. α_{ki} is a complex value which is related to the instantaneous channel state i, where r refers to the position vector and z is the propagation distance. The vector of the received field $\mathrm{Y} = [y_1, \ldots, y_N]^T$ can be expressed as

$$\mathrm{Y} = |H_\rho|^2, \tag{12}$$

$$\mathrm{H} = \begin{bmatrix} \alpha_{11} & \ldots & \alpha_{N1} \\ \vdots & \ddots & \vdots \\ \alpha_{1N} & \ldots & \alpha_{NN} \end{bmatrix}, \tag{13}$$

where H is the channel matrix and $\rho = [\rho_1, \ldots, \rho_N]^T$ is a vector of the transmitted signal. This non-linear transformation between the received power Y and transmitted signal ρ is due to the square-law detection making the conventional MIMO (CMIMO) digital signal processing (DSP) techniques [36], [37]. N is a number of transmitted spatial modes N in SMM. Using Eq. (11), the photon rate A_i for this channel can be rewritten by [35]–[37]

$$A_i = \mu \left|\rho_i \alpha_{ii} + \sum_{k \epsilon N, K \neq i} \rho_k \alpha_{ki}\right|^2, \tag{14}$$

where $\rho_i \alpha_{ii}$ refers to the signal from the calculated SMM [35], [38], [39]. We assume that the receiver has the channel state information of the signal amplitude fading $|\boldsymbol{\alpha_{ii}}|$, which estimated by collecting the received power and exciting the SMM state i in the same mode. Using the mean achievable rate (MAR) given by Eq. (17) in [40], the MAR conditioned on the signal α_{ii} can be shown as

$$\begin{aligned} \boldsymbol{C}_{(i\,|\,\boldsymbol{\alpha_{ii}})} &= \frac{1}{2}\log\frac{\mu|\alpha_{ii}|^2 P_t}{N\sigma_{z_{s.i}}^2} + \frac{1}{2}\log\left(1 + \frac{2N\sigma_{z_{s.i}}^2}{\mu|\alpha_{ii}|^2 P_t}\right) \\ &\quad - \frac{\mu|\alpha_{ii}|^2 P_t}{N\sigma_{z_{s.i}}^2} - 1 \\ &\quad + \frac{\sqrt{\mu|\alpha_{ii}|^2 P_t\left(\mu|\alpha_{ii}|^2 P_t + 2N\sigma_{z_{s.i}}^2\right)}}{N\sigma_{z_{s.i}}^2} \\ &\quad - \sqrt{\frac{\pi N\sigma_{z_{0.i}}^2}{2\mu|\alpha_{ii}|^2 P_t\sigma_{z_{s.i}}^2}}, \end{aligned} \tag{15}$$

This rate can be achieved from half-normal distributed with the probability density function is given by

$$f_\rho(\rho) = \sqrt{\frac{2N}{\pi P_t}}\exp\left(-\frac{N\rho^2}{2P_t}\right). \tag{16}$$

Since both of the noise variance $\sigma^2_{z_{s,i}}$ and $\sigma^2_{z_{0,i}}$ contain $m_{c.i}$ is the average signal photon given by $m_{c.i} = 2\mu\sigma^2_{c,i}$ which depends on the transmitted optical power P_t [35]. The asymptotic MAR at high P_t can be achieved as

$$C^{\infty}_{(i\,|\,\alpha_{ii})} = \frac{1}{2}\log\left(\frac{1}{2}\gamma_i + 2\right) - \frac{\gamma_i}{2} - 1 + \frac{\sqrt{\gamma_i\,(\gamma_i+4)}}{2} - \sqrt{\frac{\pi}{4\gamma_I}}, \quad (17)$$

The instantaneous asymptotic SNR γ_i is given by

$$\gamma_i = |\alpha_{ii}|^2 \Big/ \sum_{k\epsilon N, k\neq i} E\left[|\alpha_{ki}|^2\right]. \quad (18)$$

The received field for OAM–MIMO/SMM multiplexing i at the transmitter plane is given by [35]

$$u_i\,(w_z, \varphi, 0) = \sqrt{\frac{2}{\pi\,|\mathrm{i}|!}}\frac{1}{w_0}\left(\frac{\sqrt{2}w_z}{w_0}\right)^{|\mathrm{i}|} L^i_0\left(\frac{2w_z^2}{w_0^2}\right) \times exp\left(\frac{-w_z^2}{w_0^2}\right) exp\,(-ji\varphi)\,, \quad (19)$$

where w_0 is the beam waist for GB at the transmitter plane, L^i_0 $(\cdot)$ represents the LG polynomial and $\boldsymbol{\varphi}$ refer to the azimuthal angle.

III. ANALYSIS OF THE POWER PENALTY PERFORMANCE

We simulated for four OAM-modes multiplexed based on MIMO/SMM in the FSO communication link, with each channel is transmitting a 16-QAM signal. The transmitter apertures contain four OAM–MIMO/SMM-multiplexed, each mode is carrying a 100Gbit/s QPSK signal, resulting in four OAM channels. The error probability of a 16-QAM (Mq) signal is given as [7], [18], [41]

$$\mathrm{P_{e,16\text{-}QAM(Mq)}} = 3\mathrm{Q}\left(\sqrt{\frac{4E_{avg}}{5N_0}}\right)\left[1 - \frac{3}{4}\mathrm{Q}\left(\sqrt{\frac{4E_{avg}}{5N_0}}\right)\right], \quad (20)$$

where E_{avg}/N_0 is the average SNR per bit. E_{avg} is the average received power and N_0 is the power density of AWGN, and $Q\,(\cdot)$ is the complementary error function [7], [18], [42]. Eq. (20) allows the calculation of the minimum power required at the transmitter P_{rq} for a single channel to achieve a target BER. In our analysis, we choose a FEC limit of 3.8×10^{-3} as the BER threshold [43]. We assume that: (i) all channels have the same transmitted power; (ii) channel crosstalk interferes with the signal in a similar way as the noise at our BER threshold [, [18]. $\alpha_{rq,m}$ and $\beta_{rq,m}$ are the effective number of large-scale and small-scale eddies of the scattering process, respectively. The power penalty is defined as

$$P_{\text{penalty}} = 10 \cdot \log_{10}\left(\frac{P_{rq,m}}{P_{rq}}\right) \text{dB}. \quad (21)$$

$$P_{rq,m} = P_{rq}\left(\alpha_{rq,m} - \beta_{rq,m} \cdot \frac{P_{rq}}{N_0}\right)^{-1}, \quad (22)$$

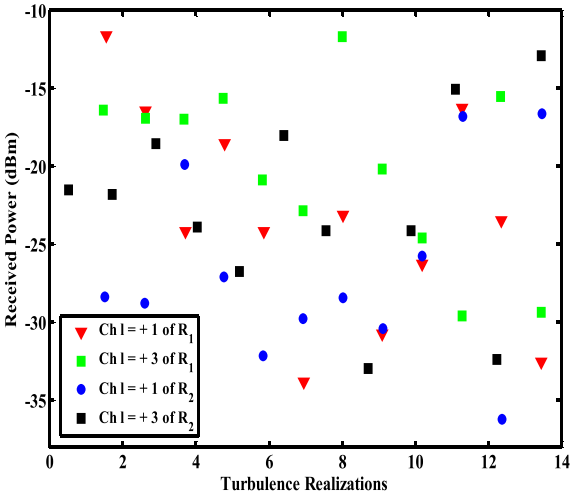

(a)

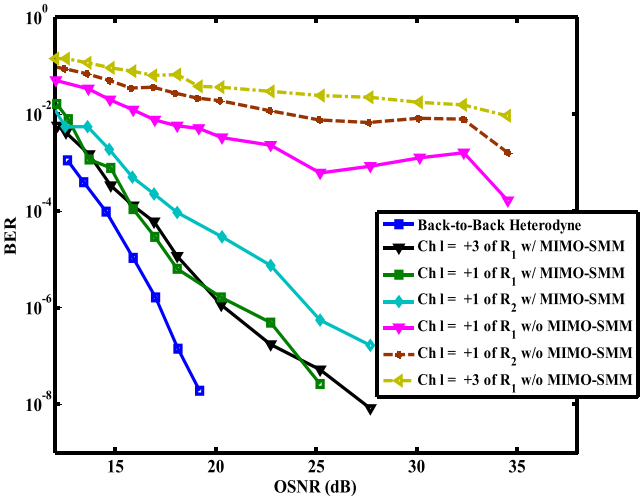

(b)

FIGURE 2. Weak turbulence (a) the received power and (b) BER curves with and without SMM/MIMO signal processing.

where $P_{rq,m}$ is the minimum power required at the transmitter for channel m can be expressed as [7], [18]. For calculations of spot size (beam diameter) D, the second moment of the intensity of an OAM beam or GBs, which is generally related to the beam waist, is employed, as given by the following equation:

$$D = 2\sqrt{\frac{2\int_0^{2\pi}\int_0^{\infty} w_0^2 I\,(w_0, \boldsymbol{\varphi})\,w_0 dw_0 d\boldsymbol{\varphi}}{\int_0^{2\pi}\int_0^{\infty} I\,(w_0, \boldsymbol{\varphi})\,w_0 dw_0 d\boldsymbol{\varphi}}}, \quad (23)$$

Here, $\boldsymbol{\varphi}$ is the azimuthal angle varying from 0 to 2π, $I\,(w_0, \boldsymbol{\varphi})$ is the radial intensity and $(w_0, \boldsymbol{\varphi})$ are polar coordinates [7].

IV. NUMERICAL RESULTS AND DISCUSSIONS

The physical parameters used in the calculations are presented in Table 1. The default parameters are implemented in Table 2. To check the credibility of the below results, OAM–MIMO/SMM in FSO links have been simulated using

TABLE 1. The physical parameters used for calculations [proposal] and ref. [18].

Parameters	Descriptions	Values [Proposal]	Values [18]
Mq	No. of QAM states	16	16
λ_{sig}	Desired signal wavelength	1550 nm	1550 nm
QPSK	Quadrature phase-shift keying signals	100 Gbit/s	20 Gbit/s
f_1, f_2	Focal lengths of transmitter lenses	0.5 m	0.5 m
l_{OAM}	No. of OAM channels	4	8
P_t	Transmitted optical power	−13 dBm	−5 dBm
l_{fso}	Maximum FSO link length	2000 m	200 m
R	Photo-detector responsivity	1 A/W	0.9 A/W
D_{Tx}	Transmitted beam size	30 cm	8 cm

TABLE 2. Design parameters required for an OAM–MIMO/SMM in FSO link.

Design Parameters	Symbols
Beam waist	w_0
Instantaneous asymptotic signal-to-interference ratio	γ_i
Radial distance	r
Azimuthal angle	φ
Transmitted beam size (diameter)	D_{Tx}
Receiver aperture size (diameter)	D_{Rx}
Generalized LG polynomial	$L_0^i(\cdot)$
Refractive index structure constant	C_n^2
Average SNR per bit	E_{avg}/N_0
Rytov variance	σ_R^2
No. of transmitted spatial modes in SMM	N

Matlab. The OAM–MIMO/SMM signal traveling through the turbulence is encountered by various AT [44], [45]. Fig. 2(a) and 2(b) show the received power and BERs under 14 turbulence realizations and BER curves as a function of OSNR with and without OAM–MIMO/SMM based DSP, respectively. It can be seen from the results [Fig. 2 (a)] that the received power fluctuates by 4.5 dB −6 dB and all BERs after MIMO-DSP are below FEC of 3.8×10^{-3} as shown in Fig. 2 (a). We can see that BER increases using an OAM–MIMO/SMM multiplexing varies for different realizations. We see that without an adaptive MIMO/SMM equalization, the BER of 10^{-9} show the "*error floor*" (EF) due to the

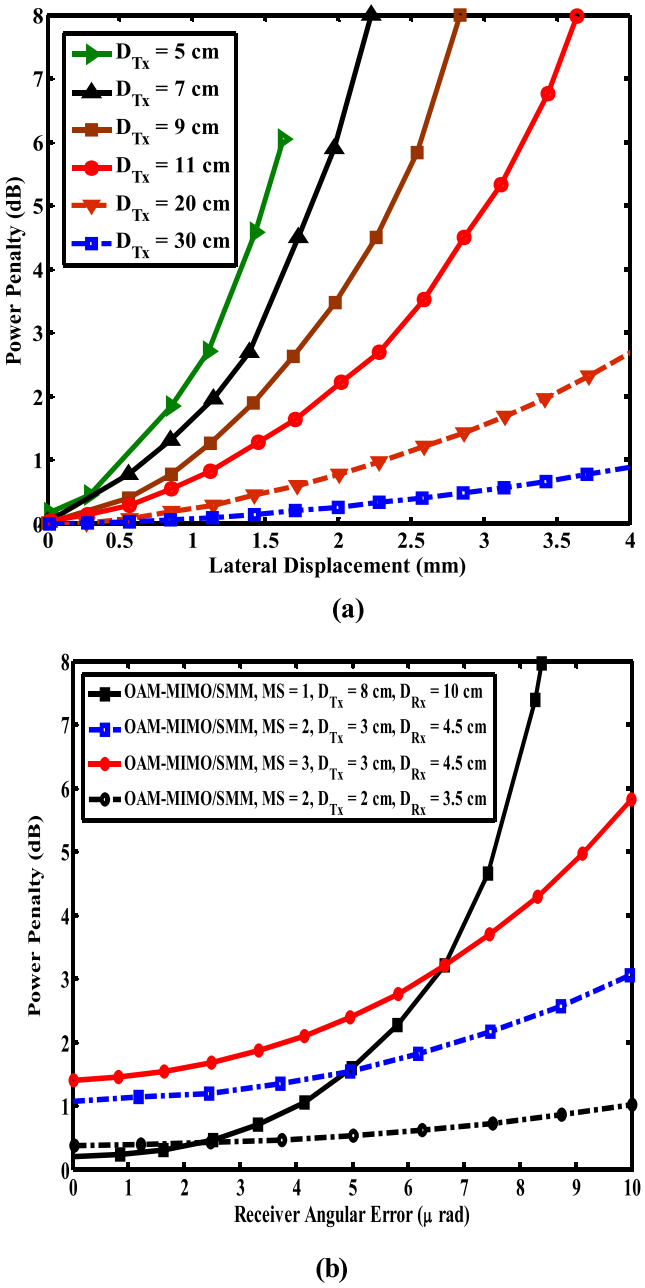

FIGURE 3. Simulated systems PP (dB) as a function of (a) lateral displacement (mm), (b) RAE (μ rad), and transmission distance are 2 km.

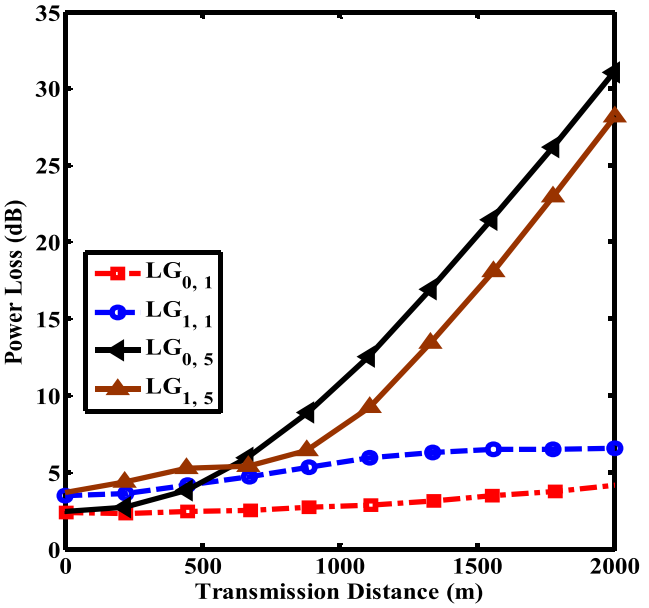

FIGURE 4. The power loss of LG beams with $\rho = 0$ and $\rho > 0$ as functions of transmission distance, with D_{Tx} of 8 cm and D_{Rx} of 10 cm.

strong turbulence (ST) and decrease after using an adaptive MIMO/SMM technique and the system PP is below 4 dB as shown in Fig. 2 (b). Fig. 3 shows the system PP for various transmitted beam sizes. When the applied lateral displacement is 2 mm, a system with $D_{Tx} = 11$ cm suffers ~ 2 dB less PP than that with $D_{Tx} = 7$ cm [see Fig. 3(a)]. Fig. 3(b) shows the results of the PP for four OAM–MIMO/SMM are transmitted over a 2 km link with different D_{Tx} and D_{Rx}. Mode spacing of 2 with $D_{Tx} = 3$ cm and $D_{Rx} = 4.5$ cm for OAM–MIMO/SMM has better performance than the MS of 1 when the RAE is larger than 5 μrad. With $D_{Tx} = 8$ cm and $D_{Rx} = 10$ cm, the PP is slightly larger than that of $D_{Tx} = 3$ cm and $D_{Rx} = 4.5$ cm for OAM–MIMO/SMM [46]. The system with MS of 2, $D_{Tx} = 2$ cm and $D_{Rx} = 3.5$ cm of OAM–MIMO/SMM beams should fulfill less PP of 1 dB as shown in Fig. 3 (b). The PP analysis indicates some selection rules for MS: (i) a larger transmitted beam size and receiver aperture could increase the system tolerance to lateral displacement, but decrease its tolerance to receiver angular error, and (ii) systems with larger MS have higher-order OAM beams, which leads to higher signal power loss due to beam divergence, however, such systems also suffer less ICC [7] as shown in Fig. 3. For example, mode spacing of 1 with $D_{Tx} = 8$ cm and $D_{Rx} = 10$ cm show higher power penalty than MS of 2 at $D_{Tx} = 2$ cm and $D_{Rx} = 3.5$cm for RAE. Comparing between Fig. 3 (a) [present work] and Fig. (5) [18] show the ICC impact and PP of OAM–MIMO/SMM. The PP can be reduced of 1 dB at a target BER of 10^{-9} [present work]. Fig. 4 shows the advantage of using $\rho > 0$ beams may also decrease under larger D_{Rx}. We simulate the power loss for different l and ρ values when $D_{Rx} = 10$ cm. It can be seen that (i) the power loss of $LG_{0,1}$ is smaller than $LG_{1,1}$at most transmission distances, which is because through the inner ring of $LG_{1,1}$ is smaller than the single ring of $LG_{0,1}$ (ii) $LG_{0,5}$ has lower power loss than $LG_{1,5}$ at < 600 m because the receiver aperture covers only part of the outer ring of $LG_{1,5}$ but covers most of the single ring of $LG_{0,5}$ [47]–[49]. Fig. 5 shows the BER as a function of average optical-SNR (OSNR). The numerical results show that without using the lenses of an adaptive MIMO/SMM, the BER curves show the EF due to ST and decrease after using the lenses [29, 43]. The outage probability (OP) versus the transmitted optical power with and without the SMD is plotted in Fig. 6 for $C_n^2 = 8.54 \times 10^{-15}\text{m}^{-2/3}$, and $C_n^2 = 1 \times 10^{-15}\text{m}^{-2/3}$, respectively. According to Rytov

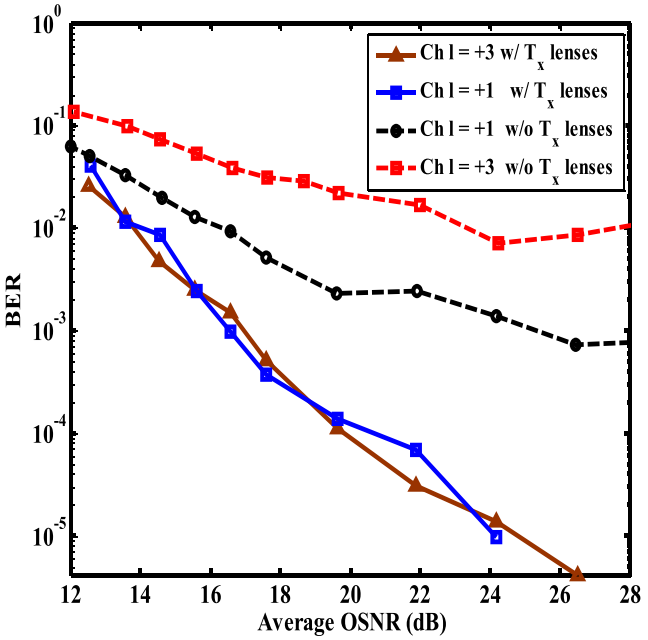

FIGURE 5. BER vs. average OSNR (dB) for two channels ($l = +1$, $l = +3$) with and without T_x lenses of OAM–MIMO/SMM multiplexing.

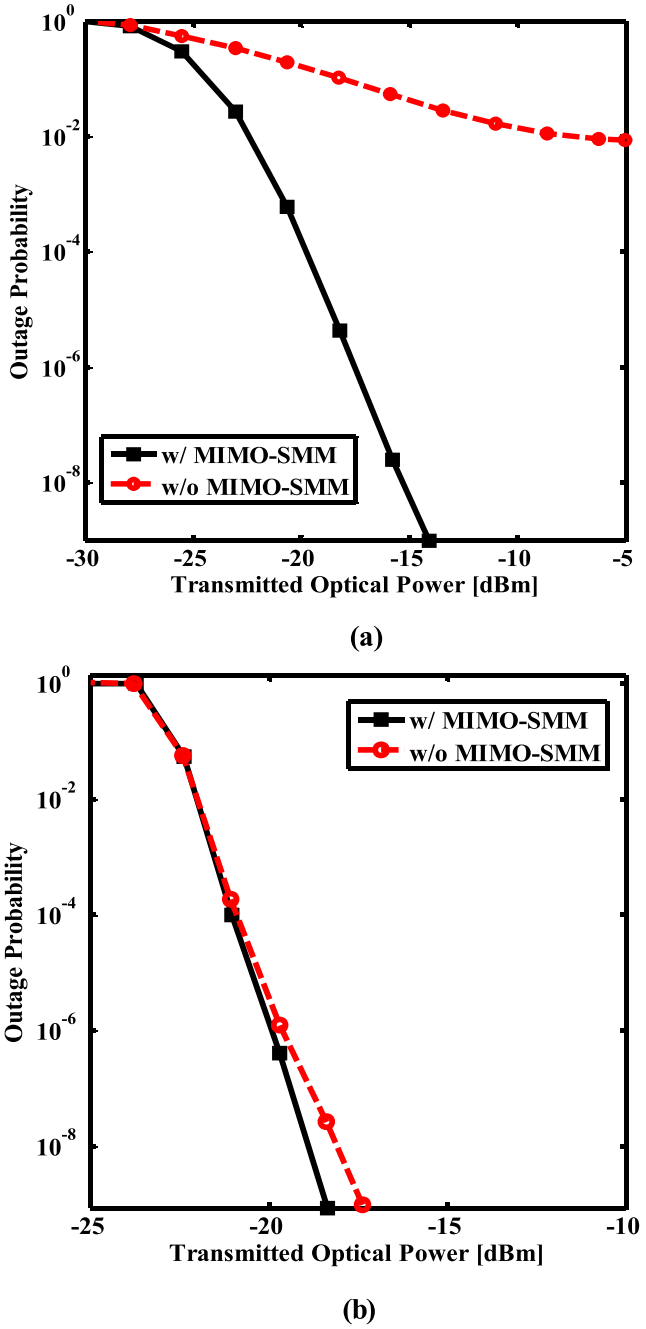

FIGURE 6. The OP versus the transmitted optical power for OAM–MIMO/SMM system with and without the SMD; (a) transmitted mode N = {±10} and $C_n^2 = 8.54 \times 10^{-15} m^{-2/3}$, (b) N = {0} and $C_n^2 = 1 \times 10^{-15} m^{-2/3}$.

variance $\sigma_R^2 = 1.23 C_n^2 k^{7/6} l_{fso}^{11/6}$ [35], [50] where the wave number $k = {}^{2\pi}/_{\lambda}$, λ is the wavelength and l_{fso} is the FSO link length. For each multiplexed channel, the best mode sets for SMD as presented in Fig. 6. From Fig. 6, we can observe the significant enhancement of the OP performance by employing the SMD. For instance, when $C_n^2 = 8.54 \times 10^{-15} m^{-2/3}$ and N = {±10}, the OP decrease to 10^{-9} in the presence of MIMO/SMM as shown in Fig. 6 (a). When the turbulence condition is $C_n^2 = 1 \times 10^{-15} m^{-2/3}$, and four modes are employed for MIMO/SMM multiplexing, the OP of the state with $i = \{0\}$ is 10^{-9} for $P_t = -18$ dBm as shown in Fig. 6 (b) [35]. In order to illustrate the performance improvements achieved by the LDPC coded OAM multiplexing, the normalized power requirements at BER of 10^{-9} [51] are shown in Fig. 7. The simulated power distributions of the OAM–MIMO/SMM beam as a function of the RAE with and without T_x lenses are depicted in Fig. 7 (a) and 7 (b), respectively. In this figure, the OAM beam of $l = +3$ is transmitted to a distance of 2 km, with D_{Tx} and D_{Rx} is 35 cm. Fig 7 (a) shows less power loss with Fig. 7 (b). The simulation results show that the use of T_x lenses could enhance the system robustness under the RAE [28]. Also, the T_x lenses used in our system will improve the transmitted power, reduced the power penalty, and enhance the system robustness. Thus, the amplifying signal of the lens will be affected by some noise, but an adaptive threshold function of the proposed system will control the noise and compensate the decreased of SNR for the lowest BER in the sent data. Fig. 8 shows the obtained BER as a function of OSNR by multiplexing 4 × 4 OAM modes for $l = +3$ channels with and without adaptive MIMO/SMM multiplexing. We extrapolated this curve to cross the FEC threshold with MIMO/SMM multiplexing at the OSNR of 15 dB at the BER of 1.763×10^{-4}. After the adaptive MIMO equalization, the estimated required OSNR at the BER of 3.8×10^{-3} is 6.5 dB. Fig. 9 compares the BER curves vs. SNR [dB] under Gamma-Gamma (GG) turbulence for different values of Rytov variance. It is observed from the figure that, as the values of σ_R^2 decreases from 3.51 to 0.63, resulting in a better BER performance of the system. This is because of the fact that larger values of σ_R^2 correspond to the case of stronger turbulence. It can also be seen from

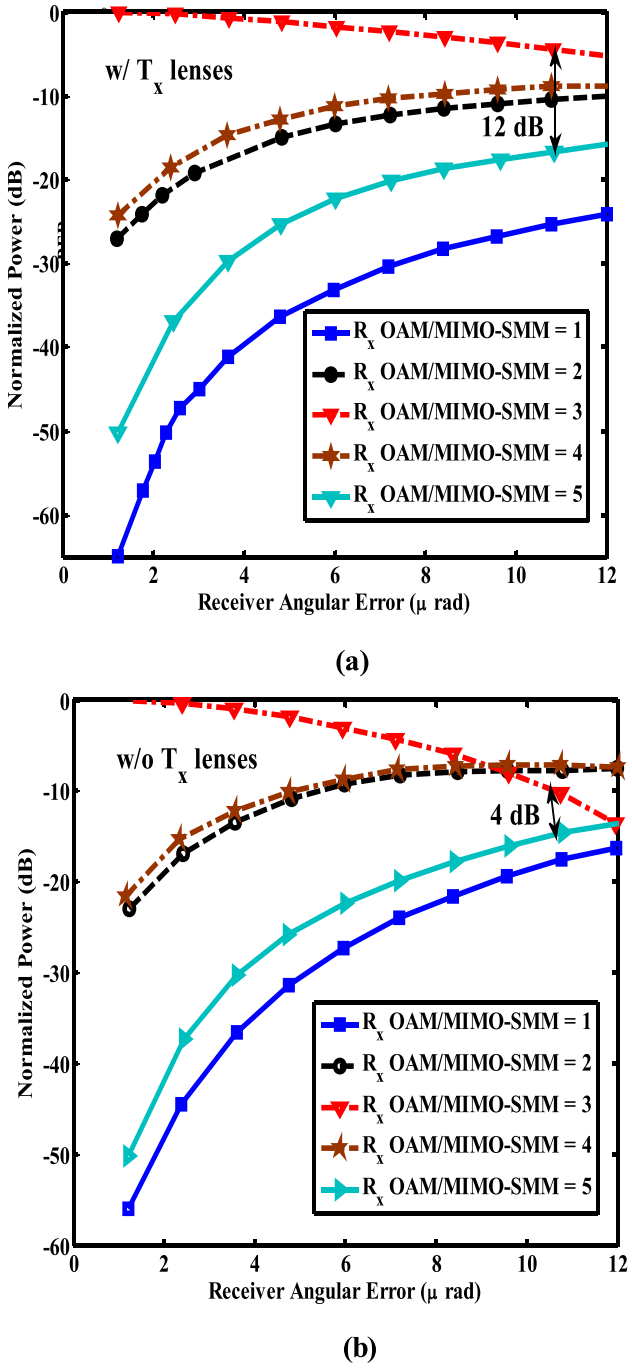

FIGURE 7. Simulated OAM–MIMO/SMM power distribution of 2-km FSO link with (a) RAE (μrad) and T_x lenses and (b) RAE (μrad) but without T_x lenses.

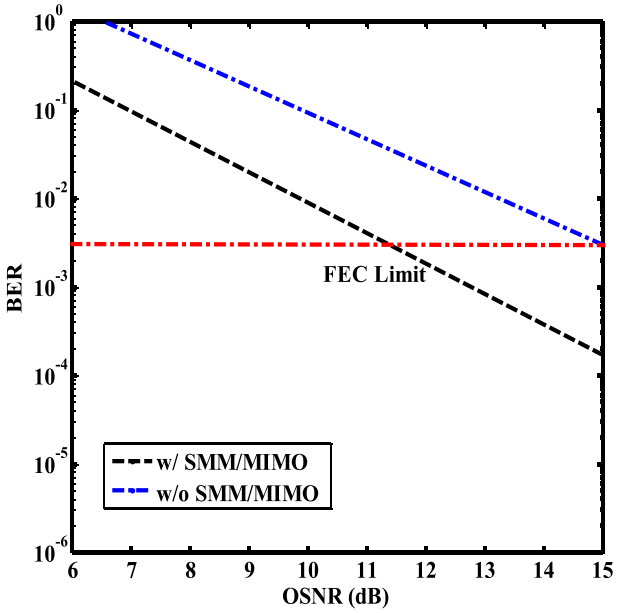

FIGURE 8. Obtained BER as a function of OSNR (dB) with multiplexing 4 × 4 OAM modes for $l = +3$ channels with and without adaptive SMM/MIMO equalization.

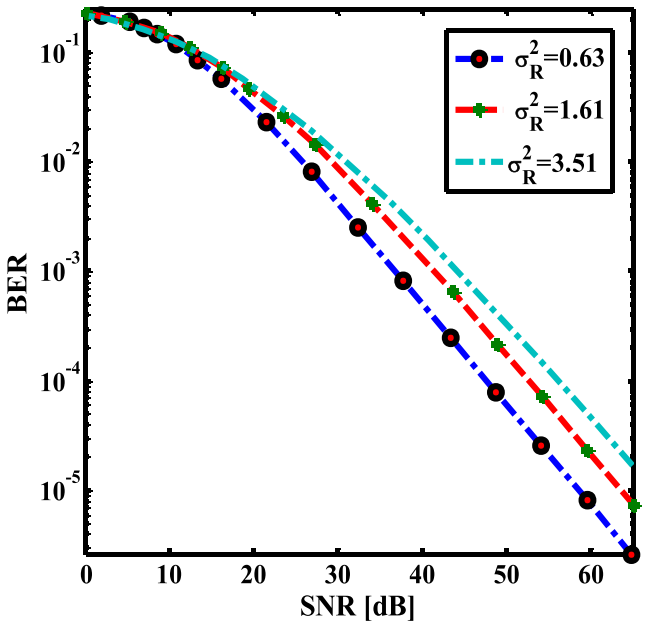

FIGURE 9. Analytical BER vs. SNR [dB] under GG turbulence for different values of Rytov variance.

Fig. 9 that, for $\sigma_R^2 = 1.61$, the BER is 2.31e−005 at 60 dB SNR and 8.1e−006 at an SNR of 65 dB. As a result, the diversity achieved is $\log_{10}(2.31e-005) - \log_{10}(8.1e-006) = 0.455$. It is observed from Fig. 9 that, for $\sigma_R^2 = 3.51$, the BER is 5.125e−005 at 60 dB SNR and 1.696e−005 at SNR 65 dB. As a result, the diversity achieved is $\log_{10}(5.125e-005) - \log_{10}(1.696e-005) = 0.480$. It can also be seen from Fig. 9 that, for $\sigma_R^2 = 0.63$, the BER is 8.1e-006 at SNR 60 dB and 2.612e−006 at SNR 65 dB and the diversity achieved is $\log_{10}(8.1e-006) - \log_{10}(2.612e-006) = 0.491$. The calculation results of Fig. 9 are summarized in Table 3. Fig. 10 shows the channel capacity as a function of the SNR (dB) for different spatial diversity in an OAM–MIMO multiplexed beams. It is observed from the figure that the OAM-based SMM/MIMO-SMD outperforms the conventional MIMO (CMIMO) by 3 dB [52]–[54]. The SMM/MIMO-SMD technique performed better in the channel capacity and SNR over other commonly used

TABLE 3. The calculation results of the BER and SNR under gamma-gamma turbulence for different values of Rytov variance.

Rytov Variance, σ_R^2	BER at 60 dB SNR	BER at 65 dB SNR	Diversity Order
$\sigma_R^2 = 3.51$	5.125e−005	1.696e−005	0.480
$\sigma_R^2 = 1.61$	2.31e−005	8.1e−006	0.455
$\sigma_R^2 = 0.63$	8.1e−006	2.612e−006	0.491

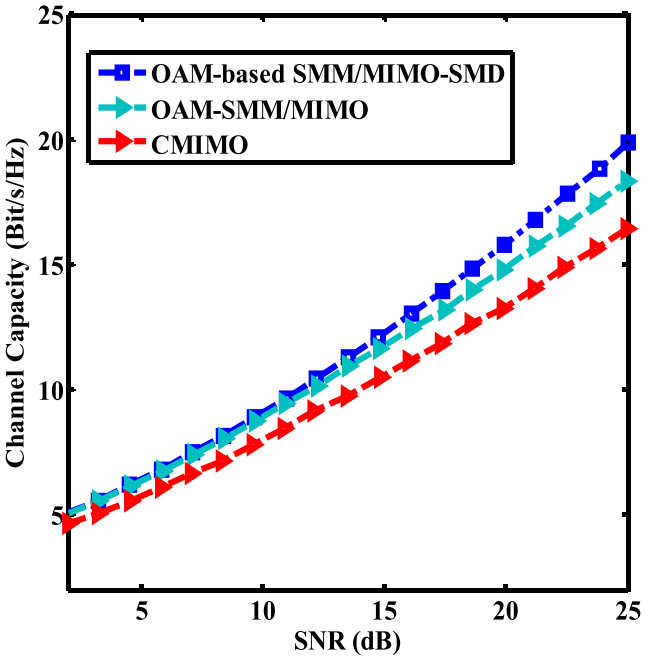

FIGURE 10. The channel capacity vs. SNR (dB) for different spatial diversity in an OAM–MIMO multiplexed beams.

CMIMO algorithms. We show that the novelty approach can improve the diversity gain and channel capacity.

V. CONCLUSIONS AND FUTURE WORK

We have investigated the high-speed of an OAM and adaptive MIMO-based SMM/SMD multiplexed free-space optical link, enabled by adaptive optics, LDPC-coded OAM-based transmission system, and SMD. The OAM–MIMO/SMM wireless optical links is a multi-element link, which exploits spatial dimensions to derive the spectral efficiency and gains in reliability. Through outage probability analysis, it is concluded that using SMD, both the OP and outage MAR can be significantly improved. The proposed system shows that the BER can reach to 10^{-9} and the power penalty of 1 dB −4 dB for all channels after OAM–MIMO/SMM equalization. The proposed system with mode spacing of 2 for four OAM–MIMO/SMM beams are transmitted over a 2 km link should fulfill less power penalty of 1 dB. The power penalties can be reduced by 1 dB − 4 dB for all channels after OAM–MIMO/SMM equalization at a BER of 10^{-9}. The numerical results show that the system using OAM-based MIMO/SMM and the SMD multiplexing achieves superior BER performance to that using the adaptive MIMO/SMM equalization, with lower or nearly the same computational complexity. The simulation models verified the superior BER performance of OAM-SMD based MIMO/SMM. The simulation results illustrate that the proposed OAM–MIMO/SMM based on the SMD approach has effectively enhanced the performance of FSO links under the atmospheric turbulence effects. The algorithm is validated by the program developed by Matlab, and the results show that the model can be accurately and effectively supported. A wavelength division multiplexing of OAM–MIMO/SMM based SMD/MDM coherent FSO system can be used to increase the data rate per wavelength and the channel capacity. Finally, it should be noted that OAM–MIMO/SMM has other applications besides communications, including micromanipulation and imaging.

A. COMPLIANCE WITH ETHICAL STANDARDS

Conflict of Interest: The authors declare that there is no conflict of interest regarding the manuscript.

REFERENCES

[1] G. Gibson, J. Courtial, M. J. Padgett, M. Vasnetsov, V. Pas'ko, S. M. Barnett, and S. Franke-Arnold, "Free-space information transfer using light beams carrying orbital angular momentum," *Opt. Express*, vol. 12, no. 22, pp. 5448–5456, 2004.
[2] I. B. Djordjevic, "Deep-space and near-Earth optical communications by coded orbital angular momentum (OAM) modulation," *Opt. Express*, vol. 19, no. 15, pp. 14277–14289, Jul. 2011.
[3] J. Wang, J.-Y. Yang, I. M. Fazal, N. Ahmed, Y. Yan, H. Huang, Y. Ren, Y. Yue, S. Dolinar, M. Tur, and A. E. Willner, "Terabit free-space data transmission employing orbital angular momentum multiplexing," *Nature Photon.*, vol. 6, pp. 488–496, Jun. 2012.
[4] A. Mair, A. Vaziri, G. Weihs, and A. Zeilinger, "Entanglement of the orbital angular momentum states of photons," *Nature*, vol. 412, pp. 313–316, Jul. 2001.
[5] F. Tamburini, E. Mari, A. Sponselli, B. Thidé, A. Bianchini, and F. Romanato, "Encoding many channels on the same frequency through radio vorticity: First experimental test," *New J. Phys.*, vol. 14, no. 3, 2012, Art. no. 033001.

[6] Y. Yan, G. Xie, M. P. J. Lavery, H. Huang, N. Ahmed, C. Bao, Y. Ren, Y. Cao, L. Li, Z. Zhao, A. F. Molisch, M. Tur, M. J. Padgett, and A. E. Willner, "High-capacity millimetre-wave communications with orbital angular momentum multiplexing," *Nature Commun.*, vol. 5, Sep. 2014, Art. no. 4876.

[7] G. Xie, L. Li, Y. Ren, H. Huang, Y. Yan, N. Ahmed, Z. Zhao, M. P. J. Lavery, N. Ashrafi, S. Ashrafi, R. Bock, M. Tur, A. F. Molisch, and A. E. Willner, "Performance metrics and design considerations for a free-space optical orbital-angular-momentum–multiplexed communication link," *Optica*, vol. 2, no. 4, pp. 357–365, 2015.

[8] Y. Ren, G. Xie, H. Huang, L. Li, N. Ahmed, Y. Yan, M. P. J. Lavery, R. Bock, M. Tur, M. A. Neifeld, R. W. Boyd, J. H. Shapiro, and A. E. Willner, "Turbulence compensation of an orbital angular momentum and polarization-multiplexed link using a data-carrying beacon on a separate wavelength," *Opt. Lett.*, vol. 40, no. 10, pp. 2249–2252, 2015.

[9] Z. Qu and I. B. Djordjevic, "500 Gb/s free-space optical transmission over strong atmospheric turbulence channels," *Opt. Lett.*, vol. 41, no. 14, pp. 3285–3288, 2016.

[10] S. Li and J. Wang, "Adaptive free-space optical communications through turbulence using self-healing Bessel beams," *Sci. Rep.*, vol. 7, Feb. 2017, Art. no. 43233.

[11] H. Huang, Y. Cao, G. Xie, Y. Ren, Y. Yan, C. Bao, N. Ahmed, M. A. Neifeld, S. J. Dolinar, and A. E. Willner, "Crosstalk mitigation in a free-space orbital angular momentum multiplexed communication link using 4×4 MIMO equalization," *Opt. Lett.*, vol. 39, no. 15, pp. 4360–4363, 2014.

[12] Y. Ren, Z. Wang, G. Xie, L. Li, Y. Cao, C. Liu, P. Liao, Y. Yan, N. Ahmed, Z. Zhao, A. Willner, N. Ashrafi, S. Ashrafi, R. D. Linquist, R. Bock, M. Tur, A. F. Molisch, and A. E. Willner, "Free-space optical communications using orbital-angular-momentum multiplexing combined with MIMO-based spatial multiplexing," *Opt. Lett.*, vol. 40, no. 18, pp. 4210–4213, 2015.

[13] M. T. Dabiri, M. J. Saber, and S. M. S. Sadough, "On the performance of multiplexing FSO MIMO links in log-normal fading with pointing errors," *IEEE/OSA J. Opt. Commun. Netw.*, vol. 9, no. 11, pp. 974–983, Nov. 2017.

[14] Z. Qu and I. B. Djordjevic, "Coded orbital angular momentum based free-space optical transmission in the presence of atmospheric turbulence," in *Proc. Asia Commun. Photon. Conf. (ACP)*, Hong Kong, Nov. 2015, pp. 19–23.

[15] H. Kaushal and G. Kaddoum, "Optical communication in space: Challenges and mitigation techniques," *IEEE Commun. Surveys Tuts.*, vol. 19, no. 1, pp. 57–96, 1st Quart., 2017.

[16] Z. Qu and I. B. Djordjevic, "Approaching terabit optical transmission over strong atmospheric turbulence channels," in *Proc. 18th Int. Conf. Transp. Opt. Netw. (ICTON)*, Trento, Italy, Jul. 2016, pp. 1–5.

[17] E. Ciaramella, Y. Arimoto, G. Contestabile, M. Presi, A. D'Errico, V. Guarino, and M. Matsumoto, "1.28 terabit/s (32×40 Gbit/s) wdm transmission system for free space optical communications," *IEEE J. Sel. Areas Commun.*, vol. 27, no. 9, pp. 1639–1645, Dec. 2009.

[18] B. B. Yousif, E. E. Elsayed, and M. M. Alzalabani, "Atmospheric turbulence mitigation using spatial mode multiplexing and modified pulse position modulation in hybrid RF/FSO orbital-angular-momentum multiplexed based on MIMO wireless communications system," *Opt. Commun.*, vol. 436, pp. 197–208, Apr. 2019.

[19] J. A. Anguita, M. A. Neifeld, and B. V. Vasic, "Turbulence-induced channel crosstalk in an orbital angular momentum-multiplexed free-space optical link," *Appl. Opt.*, vol. 47, no. 13, pp. 2414–2429, May 2008.

[20] B. Rodenburg, M. P. J. Lavery, M. Malik, M. N. O'Sullivan, M. Mirhosseini, D. J. Robertson, M. Padgett, and R. W. Boyd, "Influence of atmospheric turbulence on states of light carrying orbital angular momentum," *Opt. Lett.*, vol. 37, no. 17, pp. 3735–3737, Sep. 2012.

[21] Y. X. Ren, H. Huang, G. Xie, N. Ahmed, Y. Yan, B. I. Erkmen, N. Chandrasekaran, M. P. J. Lavery, N. K. Steinhoff, M. Tur, S. Dolinar, M. Neifeld, M. J. Padgett, R. W. Boyd, J. H. Shapiro, and A. E. Willner, "Atmospheric turbulence effects on the performance of a free space optical link employing orbital angular momentum multiplexing," *Opt. Lett.*, vol. 38, no. 20, pp. 4062–4065, Oct. 2013.

[22] I. B. Djordjevic and Z. Qu, "Coded orbital angular momentum modulation and multiplexing enabling ultra-high-speed free-space optical transmission," in *Optical Wireless Communications* (Signals and Communication Technology), M. Uysal, C. Capsoni, Z. Ghassemlooy, A. Boucouvalas, and E. Udvary, Eds. Cham, Switzerland: Springer, 2016. doi: 10.1007/978-3-319-30201-0 _16.

[23] Z. Qu and I. B. Djordjevic, "Experimental evaluation of LDPC-coded OAM based FSO communication in the presence of atmospheric turbulence," in *Proc. 12th Int. Conf. Telecommun. Mod. Satell., Cable Broadcast. Services (TELSIKS)*, Oct. 2015, pp. 117–122.

[24] G. Xie, Y. Ren, H. Huang, M. P. J. Lavery, N. Ahmed, Y. Yan, C. Bao, L. Li, Z. Zhao, Y. Cao, M. Willner, M. Tur, S. J. Dolinar, R. W. Boyd, J. H. Shapiro, and A. E. Willner, "Phase correction for a distorted orbital angular momentum beam using a Zernike polynomials-based stochastic-parallel-gradient-descent algorithm," *Opt. Lett.*, vol. 40, no. 7, pp. 1197–1200, 2015.

[25] S. Li and J. Wang, "Compensation of a distorted N-fold orbital angular momentum multicasting link using adaptive optics," *Opt. Lett.*, vol. 41, no. 7, pp. 1482–1485, Apr. 2016.

[26] G. Xie, L. Li, Y. Yan, Y. Ren, Z. Zhao, P. Liao, N. Ahmed, Z. Wang, N. Ashrafi, S. Ashrafi, R. D. Linquist, M. Tur, and A. E. Willner, "Performance metrics for a free-space communication link based on multiplexing of multiple orbital angular momentum beams with higher order radial indices," in *Proc. Conf. Lasers Electro-Opt.*, 2015, pp. 1–2, Paper JTh2A.62.

[27] L. Li, G. Xie, Y. Yan, Y. Ren, P. Liao, Z. Zhao, N. Ahmed, Z. Wang, C. Bao, A. J. Willner, S. Ashrafi, M. Tur, and A. E. Willner, "Power loss mitigation of orbital-angular-momentum-multiplexed free-space optical links using nonzero radial index Laguerre–Gaussian beams," *J. Opt. Soc. Amer. B, Opt. Phys.*, vol. 34, pp. 1–6, 2017.

[28] L. Li, G. Xie, Y. Ren, N. Ahmed, H. Huang, Z. Zhao, P. Liao, M. P. J. Lavery, Y. Yan, C. Bao, Z. Wang, A. J. Willner, N. Ashrafi, S. Ashrafi, M. Tur, and A. E. Willner, "Orbital-angular-momentum-multiplexed free-space optical communication link using transmitter lenses," *Appl. Opt.*, vol. 55, no. 8, pp. 2098–2103, 2016.

[29] Y. Ren, Z. Wang, G. Xie, L. Li, A. J. Willner, Y. Cao, Z. Zhao, Y. Yan, N. Ahmed, N. Ashrai, S. Ashrafi, R. Bock, M. Tur, and A. E. Willner, "Demonstration of OAM-based MIMO FSO link using spatial diversity and MIMO equalization for turbulence mitigation," in *Proc. Opt. Fiber Commun. Conf. Exhib. (OFC)*, (OFC), Anaheim, CA, USA, Mar. 2016, pp. 1–3.

[30] R. L. Phillips and L. C. Andrews, "Spot size and divergence for Laguerre Gaussian beams of any order," *Appl. Opt.*, vol. 22, no. 5, pp. 643–644, 1983.

[31] L. C. Andrews, R. L. Phillips, and A. R. Weeks, "Propagation of a Gaussian-beam wave through a random phase screen," *Wave Random Media*, vol. 7, no. 2, pp. 229–244, 1997.

[32] L. Zou, L. Wang, C. Xing, J. Cui, and S. Zhao, "Turbulence mitigation with MIMO equalization for orbital angular momentum multiplexing communication," in *Proc. 8th Int. Conf. Wireless Commun. Signal Process. (WCSP)*, Yangzhou, China, Oct. 2016, pp. 1–4.

[33] C. Yang, C. Xu, W. Ni, Y. Gan, J. Hou, and S. Chen, "Turbulence heterodyne coherent mitigation of orbital angular momentum multiplexing in a free space optical link by auxiliary light," *Opt. Express*, vol. 25, no. 21, pp. 25612–25624, 2017.

[34] Y. Li, K. Morgan, W. Li, J. K. Miller, R. Watkins, and E. G. Johnson, "Multi-dimensional QAM equivalent constellation using coherently coupled orbital angular momentum (OAM) modes in optical communication," *Opt. Express*, vol. 26, no. 23, pp. 30969–30977, 2018.

[35] S. Huang, G. R. Mehrpoor, and M. Safari, "Spatial-mode diversity and multiplexing for FSO communication with direct detection," *IEEE Trans. Commun.*, vol. 66, no. 5, pp. 2079–2092, May 2018.

[36] Y. Yadin and M. Orenstein, "Parallel optical interconnects over multimode waveguides using mutually coherent channels and direct detection," *J. Lightw. Technol.*, vol. 25, no. 10, pp. 3126–3131, Oct. 2007.

[37] S. Arik and J. M. Kahn, "Direct-detection mode-division multiplexing in modal basis using phase retrieval," *Opt. Lett.*, vol. 41, no. 18, pp. 4265–4268, Sep. 2016.

[38] N. W. Bikhazi, M. A. Jensen, and A. L. Anderson, "MIMO signaling over the MMF optical broadcast channel with square-law detection," *IEEE Trans. Commun.*, vol. 57, no. 3, pp. 614–617, Mar. 2009.

[39] S. O. Arik and J. M. Kahn, "Low-complexity implementation of convex optimization-based phase retrieval," Jul. 2017, *arXiv:1707.05797*. [Online]. Available: https://arxiv.org/abs/1707.05797#

[40] S. M. Moser, "Capacity results of an optical intensity channel with input-dependent Gaussian noise," *IEEE Trans. Inf. Theory*, vol. 58, no. 1, pp. 207–223, Jan. 2012.

[41] J. Proakis and M. Salehi, *Digital Communications*, 5th ed. New York, NY, USA: McGraw-Hill, 2007.

[42] G. A. Turnbull, D. A. Robertson, G. M. Smith, L. Allen, and M. J. Padgett, "The generation of free-space Laguerre–Gaussian modes at millimetre-wave frequencies by use of a spiral phaseplate," *Opt. Commun.*, vol. 127, nos. 4–6, pp. 183–188, 1996.
[43] *Forward Error Correction for High Bit-Rate DWDM Submarine Systems*, document ITU-T Rec. G.975.1, 2004.
[44] J. Jeyaseelan, D. S. Kumar, and B. E. Caroline, "PolSK and ASK modulation techniques based BER analysis of WDM-FSO system for under turbulence conditions," *Wireless Pers. Commun.*, vol. 103, no. 4, pp. 3221–3237, 2018.
[45] H. Nouri and M. Uysal, "Adaptive MIMO FSO communication systems with spatial mode switching," *J. Opt. Commun. Netw.*, vol. 10, no. 8, pp. 686–694, 2018.
[46] L. Zou, L. Wang, and S. Zhao, "Turbulence mitigation scheme based on spatial diversity in orbital-angular-momentum multiplexed system," *Opt. Commun.*, vol. 400, pp. 123–127, Oct. 2017. [Online]. Available: https://nusearch.nottingham.ac.uk/primo-explore/fulldisplay?docid=TN_sciversesciencedirect_elsevierS0030-4018(17)30401-7&context=PC&vid=44NOTUK&lang=en_US&search_scope=44NOTUK_COMPLETE&adaptor=primo_central_multiple_fe&tab=44notuk_complete&query=any,contains,FSO%20orbital%20angular%20momentum&mode=Basic
[47] M. Li, Y. Takashima, X. Sun, Z. Yu, and M. Cvijetic, "Enhancement of channel capacity of OAM-based FSO link by correction of distorted wavefront under strong turbulence," in *Proc. Frontiers Opt., Tech. Dig.*, Tucson, AZ, USA, Oct. 2014, Paper FTh3B.6. doi: 10.1364/FIO.2014.FTh3B.6.
[48] M. A. Porras, R. Borghi, and M. Santarsiero, "Relationship between elegant Laguerre–Gauss and Bessel–Gauss beams," *J. Opt. Soc. Amer. A, Opt. Image Sci.*, vol. 18, no. 1, pp. 177–184, 2001.
[49] N. Chandrasekaran and J. H. Shapiro, "Photon information efficient communication through atmospheric turbulence—Part I: Channel model and propagation statistics," *J. Lightw. Technol.*, vol. 32, no. 6, pp. 1075–1087, Mar. 15, 2014.
[50] L. Andrews and R. Phillips, *Laser Beam Propagation Through Random Media*. Bellingham, WA, USA: SPIE, 2005.
[51] Z. Qu and I. B. Djordjevic, "Orbital angular momentum multiplexed free-space optical communication systems based on coded modulation," *Appl. Sci.*, vol. 8, no. 11, p. 2179, 2018.
[52] L. Wang, F. Jiang, M. Chen, H. Dou, G. Gui, and H. Sari, "Interference mitigation based on optimal modes selection strategy and CMA-MIMO equalization for OAM-MIMO communications," *IEEE Access*, vol. 6, pp. 69850–69859, 2018.
[53] D. Lee, H. Sasaki, H. Fukumoto, Y. Yagi, T. Kaho, H. Shiba, and T. Shimizu, "An experimental demonstration of 28 GHz band wireless OAM-MIMO (orbital angular momentum multi-input and multi-output) multiplexing," in *Proc. IEEE 87th Veh. Technol. Conf. (VTC Spring)*, Porto, Portugal, Jun. 2018, pp. 1–5. doi: 10.1109/VTCSpring.2018.8417790.
[54] D. Lee, H. Sasaki, H. Fukumoto, Y. Yagi, and T. Shimizu, "An evaluation of orbital angular momentum multiplexing technology," *Appl. Sci.*, vol. 9, no. 9, p. 1729, Apr. 2019. doi: 10.3390/app9091729.

BEDIR BEDIR YOUSIF received the B.Sc. degree in electronics engineering from the Faculty of Electronic Engineering, Menoufia University, Egypt, in 1999, and the M.Sc. and Ph.D. degrees from the Department of Electronics and Communications Engineering, Faculty of Engineering, Mansoura University, Mansoura, Egypt, in 2006 and 2013, respectively. He is currently an Associate Professor with the Electronics and Communications Engineering Department, Faculty of Engineering, Kafrelsheikh University, Kafrelsheikh, Egypt. He has several publications in the modeling of plasmonic devices, optical communications, optoelectronic devices, nano-electronics, and antennas. His research and teaching interests include the areas of optical wireless communications, the modeling of electromagnetic devices, nano-electronics, optical devices, and optical communications.

EBRAHIM ELDESOKY ELSAYED received the B.Sc. degree in electronics and communications engineering from the Misr Higher Institute for Engineering and Technology, Mansoura, Egypt, in 2012, and the Diploma degree (high Diploma) in engineering applications of laser (EAL) from the National Institute of Laser Enhanced Sciences (NILES), Cairo University, Giza, Egypt, in 2017. He is currently pursuing the M.Sc. degree in electrical communications engineering with the Electronics and Communications Engineering Department, Faculty of Engineering, Mansoura University, Mansoura. His research interests include the areas of optical wireless communications, free-space optical communications, optoelectronic devices, optical devices, and MIMO wireless communication systems.